

# Acoustic backscattering by Hawaiian lutjanid snappers.

## I. Target strength and swimbladder characteristics

Kelly J. Benoit-Bird and Whitlow W. L. Au<sup>a)</sup>

Hawaii Institute of Marine Biology, University of Hawaii, P.O. Box 1106, Kailua, Hawaii 96734

Christopher D. Kelley

Hawaii Undersea Research Laboratory, University of Hawaii, Honolulu, Hawaii 96822

(Received 13 September 2002; accepted for publication 11 August 2003)

The target strengths and swimbladder morphology of six snapper species were investigated using broadband sonar, x rays, and swimbladder casts. Backscatter data were obtained using a frequency-modulated sweep (60–200 kHz) and a broadband, dolphinlike click (peak frequency 120 kHz) from live fish, mounted and rotated around each of their three axes. X rays revealed species-specific differences in the shape, size, and orientation of the swimbladders. The angle between the fish's dorsal aspect and the major axis of its swimbladder ranged from 3° to 12° and was consistent between individuals within a species. This angle had a one-to-one relationship with the angle at which the maximum dorsal aspect target strength was measured ( $r^2=0.93$ ), regardless of species. Maximum dorsal aspect target strength was correlated with length within species. However, the swimbladder modeled as an air-filled prolate spheroid with axes measured from the x rays of the swimbladder predicted maximum target strength significantly better than models based on fish length or swimbladder volume. For both the dorsal and lateral aspects, the prolate spheroid model's predictions were not significantly different from the measured target strengths (observed power >0.75) and were within 3 dB of the measured values. This model predicts the target strengths of all species equally well, unlike those based on length. © 2003 Acoustical Society of America. [DOI: 10.1121/1.1614256]

PACS numbers: 43.30.Sf [WMC]

Pages: 2757–2766

### I. INTRODUCTION

The Hawaiian bottomfish fishery is comprised of 12 species, the most important of which are seven snappers in the family Lutjanidae that dwell near the bottom in deepwaters (100–400 m). Although all of these species are federally managed, two species, the onaga or long-tailed red snapper (*Etelis coruscans*) and the ehu or red snapper (*Etelis carbunculus*), have become depleted in the main Hawaiian Islands. A third species, the opakapaka or pink snapper (*Pristipomoides filamentosus*), is considered critical to the fishery (Western Pacific Regional Fisheries Management Council, 1999). These three species, the most commercially important bottomfish, are the primary species of concern in this study. Preliminary management efforts for these species have been made; however, the potential effectiveness is undetermined because very little is known about these deepwater fish and their habitat.

The use of various types of acoustic instrumentation such as side-scan sonar, split beam sonar, multi-beam sonar, and doppler current profile sounders could potentially be used to address the problems of monitoring these deepwater fish. However, all of these acoustic technologies share some common and unique disadvantages, one of which is the need for detailed acoustic backscattering data for targeted species (MacLennan, 1990). Field application of acoustic methods to estimate animal abundance requires information on the

acoustic size, target strength or backscattering cross section of individual organisms (MacLennan, 1990; Thiebaux *et al.*, 1991). No dorsal aspect measurements of acoustic scattering strength are available for deepwater snappers.

Swimbladders have been identified as the primary cause of acoustic backscattering in several species (Clay and Horne, 1994; Foote, 1980), accounting for as much as 90%–95% of echo energy. Some studies have found that the scattering field for the entire fish can be reconstructed mainly from the properties of the swimbladder (Clay and Horne, 1994; Foote, 1980; Foote and Ona, 1985). However, no information on the size, shape, or other characteristics of the swimbladders of Lutjanid snappers is available.

The objectives of Part I of this work were to obtain target strength and physiological data that could contribute to the acoustic assessment of Hawaiian deepwater snappers in the field. Measurements of backscatter strength taken *in situ* from a manned submersible show that the shape and size of the swimbladder is roughly conserved in these fish (Benoit-Bird *et al.*, 2003). However, these backscatter measurements are only from the lateral aspect of the fish. The first objective was to obtain controlled measurements of acoustic backscatter strength from all aspects of these fish, particularly the two depleted species and the pink snapper, which is the most commercially valuable species. The second was to measure the shape, size, and orientation of the swimbladders of the same fish. Objective three was to assess how acoustic backscattering strength was related to the swimbladder measures and other physiological characters such as length, biovolume, and wet weight.

<sup>a)</sup> Author to whom correspondence should be addressed. Electronic mail: wau@hawaii.edu

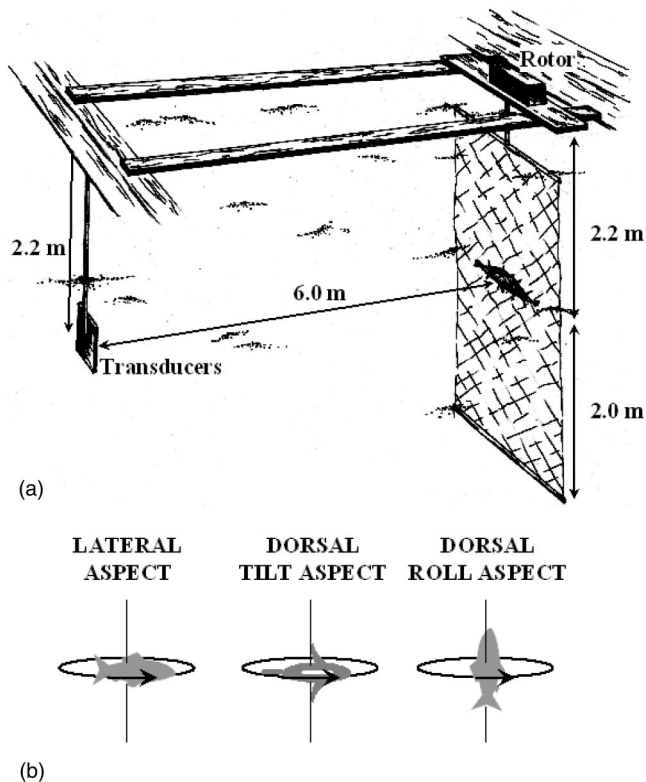


FIG. 1. (a) Experimental setup showing the position of the fish tied into a net bag and mounted to a larger, weighted net turned by a rotor. Both the transmit and receive transducer were located 6 m from the fish, 2.2 m deep, the same depth as the fish. (b) Orientations of target fish as they were rotated about their axes.

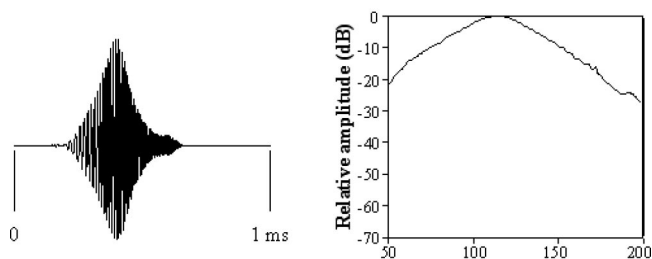
## II. METHODS

### A. Backscatter

Specimens of five of the seven Hawaiian deepwater snapper species and one introduced shallow water snapper were captured off the coasts of the Hawaiian Islands using standard, bottomfishing techniques. The fish were kept alive by immediately deflating their over-expanded swimbladders with a hypodermic needle, releasing the pressure caused by the rapid change in depth. Fish were then transported to the Hawaii Institute of Marine Biology's bottomfish hatchery on Oahu. There, they were maintained in tanks or net pens for a minimum of 8 days to allow them to acclimate to ambient conditions and heal their swimbladders before their backscattering properties were measured. A live, individual fish that had been starved for one day was then transferred into a bath containing 1 mL of 2-phenoxy-ethanol per 10 L of seawater. Once anesthetized, the fish was enclosed in a fitted monofilament net bag to restrain its movements. The net bag was mounted to a large, weighted, monofilament net that could be rotated 360° by a rotor [Fig. 1(a)]. The fish was sequentially mounted in three orientations, the order of which was randomized, for rotation about each of its three axes [dorsal tilt, dorsal roll, and lateral, Fig. 1(b)]. Ten to 11 specimens each of the three primary species of bottomfish were acoustically examined while their stomachs were empty.

A bi-static system was used to measure the echoes from the fish. Planar circular transducers were used as the projec-

### FREQUENCY MODULATED (FM) SWEEP



### DOLPHIN-LIKE CLICK

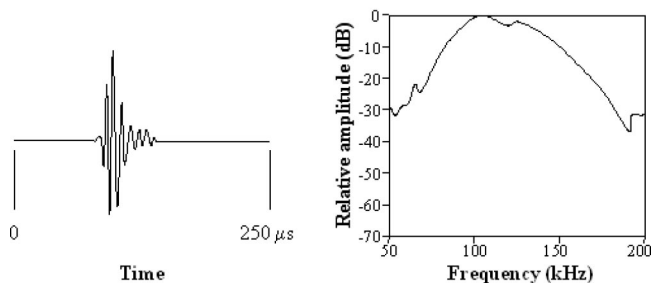


FIG. 2. Waveforms and spectrograms of the incident sonar signals.

tor and receiving hydrophone. The transducers were located side by side with a center-to-center separation distance of 10.5 cm. The transmit and receive transducers were both set up 2.2 m deep, the same depth as the mounted fish, approximately 6 m from the fish. Two signals were used, a linear, frequency-modulated sweep with a frequency range of 60 to 200 kHz and a broadband, dolphinlike click with a peak frequency of 120 kHz and a 60-kHz bandwidth, as shown in Fig. 2. The overall 3-dB beamwidth of the transducer assembly at the peak frequency of the signals was 12°. The outgoing signals were produced using a function generator computer plug-in board. The function generator also produced a trigger signal for each transmission. After a delay related to the two-way travel time from the signal to the target, a delayed trigger prompted a Rapid System R1200 analog-to-digital (A/D) converter to digitize and store a block of 1024 sample. Sampling rates of 1 MHz were used for the function generator and the A/D converter. The delayed trigger also caused the rotor and net to advance by an incremental angle. Echoes were collected in 1.5°–2.5° increments about each of the fish's three axes for both source signals.

The incident signals were first measured and digitized with the receiving hydrophone located at the position of a target fish, directly facing the projecting transducer. Target strength based on the signal amplitudes as a function of frequency was calculated by comparing the reflected signal to the incident signal using the equation

$$TS(f) = 20 \log \left[ \frac{|V_e(f)|}{|V_i(f)|} \right] + 20 \log(R), \quad (1)$$

where  $|V_e(f)|$  is the absolute value of the Fourier transform of the echo voltage after correcting for gain,  $|V_i(f)|$  is the absolute value of the Fourier transform of the incident volt-

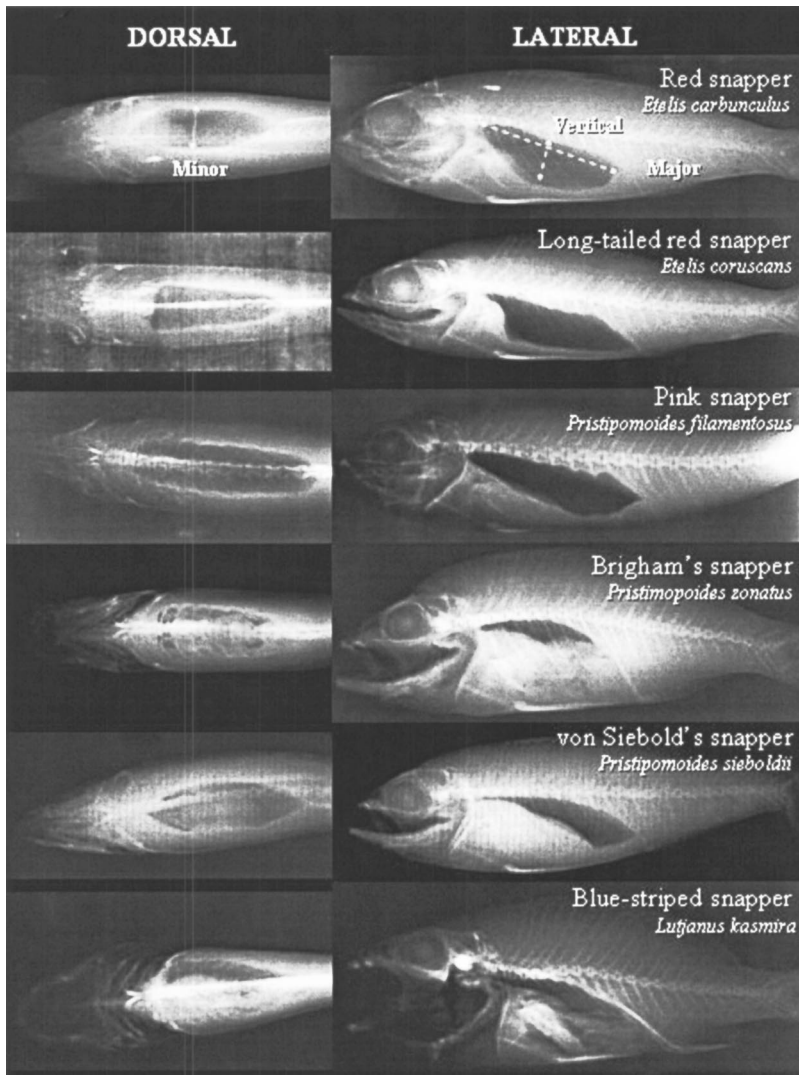


FIG. 3. Dorsal and lateral x rays of five species of Hawaiian, lutjanid snappers. The swimbladders of each fish are evident as the dark areas behind the eye and below the spine of each fish. Fish are all scaled to the same length to permit comparison of interspecies differences in swimbladder size. The axes of the swimbladder of each fish were measured from the x rays, as shown in the top panel.

age, and  $R$  is the distance between the transducers and the target. Target strength based on the energy in the incident and echo signals were also calculated using the equation

$$TS_E(f) = 10 \log[E_e/E_i] + 20 \log R, \quad (2)$$

where  $E$  is the value of the integral with respect to time of the respective instantaneous voltage squared. Target strength based on the absolute value of the voltage in the frequency domain was calculated at frequencies of 60, 100, 150, and 200 kHz using Eq. (1) and on energy using Eq. (2). Echoes from the empty net apparatus were also measured at different orientations. The net apparatus echoes interfered with the fish echoes only within  $\pm 15^\circ$  of the head and tail of the fish. Echoes from these orientations were removed from the analyses.

After acoustic measurement, fish were sacrificed by over-anesthetization using 2 mL of 2-phenoxy-ethanol per 10 L of seawater. The standard length, total length, displacement volume, and wet weight of each fish were measured after which specimens were immediately frozen.

## B. Swimbladders

Frozen fish were taken to Queen's Medical Center where they were x-rayed from both their dorsal and lateral aspects.

The lengths of each of the axes of the swimbladder and the angle between the dorsal aspect of the fish and the major axis of the swimbladder were measured directly from the x rays (Fig. 3). X rays also revealed swimbladders that were damaged during decompression. In these fish, air was evident in other cavities within the body and the bottom edge of the swimbladder was indistinct. These fish were not included in the acoustic or swimbladder analyses.

After x-raying, fish were partially thawed and a small slit was made on their ventral side to expose the ventral-most portion of the swimbladder. A syringe with an 18-gauge needle was used to inject Plaster of Paris (2 parts plaster to 1 part water) into the swimbladders following the general technique of Do and Surti (1990). A small amount of food coloring was mixed into the plaster to allow it to be seen through the translucent swimbladder wall, making it easier to determine when the swimbladders were full. When injected, the fish were partly frozen which maintained the structures around the swimbladders, preserving their shape as much as possible. The fish were refrigerated for 24 h postinjection after which the hardened swimbladder casts were extracted. Each cast was then sealed with a spray varnish and its displacement volume measured.

### C. Data analysis

The correlation between the target strengths measured using the two signal types was tested using a linear correlation. The relationships between the log of fish standard length and maximum target strength from both the dorsal and lateral aspects were assessed using a linear regression for the frequency-modulated sweep's total energy and four discrete frequencies: 60, 100, 150, and 200 kHz. The relationship between the angle at which the maximum dorsal aspect target strength was measured and the angle of the swimbladder relative to the dorsal aspect of the fish was tested with a linear regression. *F*-tests were used to test the significance of each regression's slope.

The measured maximum dorsal and lateral aspect target strengths were compared to the predictions from various simple models. First, the maximum measured target strength was compared to the target strength of the fish predicted by modeling the swimbladder as a prolate spheroid (Furusawa, 1988) using the equation

$$TS_{\text{prolate spheroid}} = 10 \log[(bc/2a)^2], \quad (3)$$

where *a*, *b*, and *c* are the axes of the swimbladder measured from the x rays and the source is parallel to axis-*a* (Urlick, 1983). The target strength derivation of Furusawa (1988) for the prolate spheroid was used instead of Stanton's (1989), mainly because of its simplicity. The second model predicts target strength of the fish by modeling the swimbladder as a sphere with a volume equivalent to that measured from the plaster cast of the swimbladder using the equation

$$TS_{\text{sphere}} = 10 \log(r^2/4), \quad (4)$$

where *r* is the radius of the sphere (Urlick, 1983). The equation for backscatter from a gas-filled sphere is considerably more complicated than Eq. (4), yet for *ka* > 1, the results are similar (Stanton, 1989). While the spherical model is a gross oversimplification of a fish, its use by commercial echosounders and in inverse techniques merits its comparison with other models. The final models for dorsal-aspect target strength are based on fish length using the equation Love (1970) developed for many types of fish and Foote's (1980) equation for swimbladder-bearing fish. Although many models of dorsal-aspect target strength of fish have been developed, those of Love (1970) and Foote (1980) are very consistent with these other models (McClatchie *et al.*, 1996). The differences between the measured and predicted target strength for each model were compared using paired *t*-tests, corrected for multiple comparisons using the Bonferroni method.

## III. RESULTS

### A. Swimbladders

The shape of the swimbladder of each species is unique and conserved between the various individual specimens of the primary species over a range of sizes (Fig. 3). Comparison of x rays to similar views of plaster casts of the swimbladders reveals that the shape of the swimbladder is con-

served by the casts. Axes measurements of the swimbladders taken with vernier calipers were within 3 mm of those taken directly from x rays.

From the lateral view, the pink snapper's swimbladder is shaped like an unbalanced ovoid with the posterior end larger than the anterior. The wider, posterior, end of the swimbladder reaches a small peak near the center of the rounded portion. From the dorsal view, the pink snapper's swimbladder is a nearly perfect ovoid, symmetrical from side to side and from front to back.

The dorsal side of the swimbladder of the red snapper is similar to that of the pink snapper, while its ventral side was much fuller after the anterior quarter. The red snapper's swimbladder, like the pink snapper's, ends in a small peak at the center of the rounded portion. From the dorsal view, the red snapper's swimbladder was nearly ovoid in shape, wider at the posterior than anterior end. Both the anterior and posterior ends of the red snapper's swimbladder taper rapidly to a point.

The long-tailed red snapper has a much more linear swimbladder than either the red snapper or the pink snapper, shaped like a rough parallelogram from the side, similar to a saddle. From the dorsal view, the red snapper's swimbladder is nearly triangular in shape, wide and flat at the anterior end and tapering to the rounded posterior end.

Plaster casts revealed three-dimensional structure that could not be observed in x rays. The pink snapper and the red and long-tailed red snapper's swimbladders have significant rippling on their dorsal and lateral sides. As many as eight bumps on the dorsal side of the swimbladders and eight corresponding diagonal grooves on the sides of the swimbladders are evident. This feature appears to be formed by the swimbladder pushing against muscles that are attached to the spine of the fish. These ripples are not evident in the Brigham's snapper, the blue-striped snapper, or von Siebold's snapper.

The standardized volume of the swimbladder (i.e., the percent of the fish's body volume) showed species-specific differences (Table I). Intraspecific variation was similar to that observed by Ona (1990). The standardized lengths of the axes of the swimbladder (i.e., the percent of the fish's body length) taken together also showed species-specific differences. The swimbladder of the blue-striped snapper and Brigham's snapper were the most distinctive because of their relatively small overall bladder size. Intraspecific variation in the relative sizes of these axes seemed to be related to the fullness of the gut. In particular, the swimbladders of fish with full stomachs were dorso-ventrally flattened, increasing the length of the minor axis and decreasing the length of the vertical axis. This affected the lateral-aspect swimbladder cross-sectional area more than the dorsal-aspect area.

The orientation of the swimbladder relative to the dorsal aspect of the fish was also species-specific. In all six fish species, the swimbladder was tilted backwards from the dorsal aspect of the fish; the anterior end of the swimbladder was higher than the posterior end. Again, the blue-striped snapper and the Brigham's snapper were the most different from the other species; their swimbladders were only slightly angled relative to the fish's dorsal aspect. The three primary

TABLE I. Characteristics of snapper swimbladders.

Species	Local common name	English common name	n	% Body length									% Body volume			Angle		
				Major			Vertical			Minor								
				mean	min	max	mean	min	max	mean	min	max	mean	min	max	mean	min	max
<i>Etelis carbunculus</i>	Ehu	Red	10	24.7	20	36	6.7	3.6	10	6.5	4.6	11	3.6	2.7	6.3	12.2	7	14
<i>Etelis coruscans</i>	Onaga	Long-tailed red	10	35.7	32	41	9.7	6.7	14	8.6	6.3	12	5.2	4.6	8.1	8.4	8	9
<i>Pristipomoides filamentosus</i>	Opakapaka	Pink	11	33.5	23	34	9.3	5.6	14	9.5	6.2	13	3.3	2.9	5.2	10.6	8	12
<i>Pristipomoides zonatus</i>	Gindai	Brigham's	1	30.8			5.2			9			1			1.5		
<i>Pristipomoides sieboldii</i>	KaleKale	von Siebold's	1	23			7			5.9			2.4			14		
<i>Lutjanus kasmira</i>	Taape	Blue-striped	1	23.1			7			5.6			1			3		

species had mean swimbladder angles that varied between 8.4° and 12.2° with the red snapper's swimbladder having the largest angle (Table I).

### B. Target strength

The angle at which the maximum dorsal-aspect target strength was measured had a nearly one-to-one relationship (slope=1,  $p > 0.10$ , power=0.93) with the angle of the swimbladder relative to the dorsal aspect of the fish, regardless of species ( $r^2 = 0.88$ ) (Fig. 4). The points that show the most difference between the two measures are the blue-striped snapper and the Brigham's snapper, both having rounded dorsal surfaces to their swimbladders and a small angle between their swimbladder and their dorsal aspect.

The total energy dorsal aspect target strengths measured with the frequency-modulated and dolphinlike signals had a strong relationship ( $r^2 = 0.89$ ) the slope of which was not significantly different from 1 ( $p > 0.10$ , power=0.86). The same is true of the lateral aspect target strengths ( $r^2 = 0.84$ ,  $p > 0.10$ , power=0.83). The echoes resulting from the frequency-modulated signal, which has a broader frequency range, are presented. For each of the three primary species, there was a strong, linear relationship between the log of the

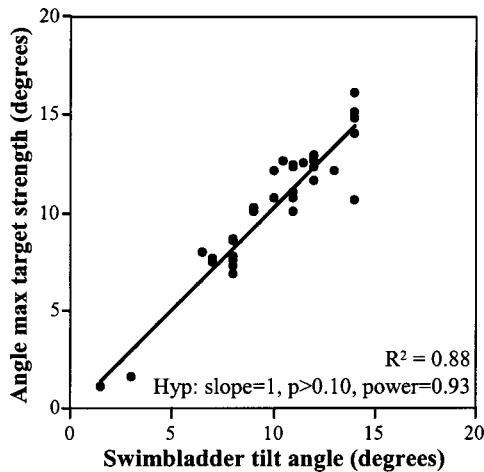


FIG. 4. Relationship between the angle of the swimbladder of each fish relative to its dorsal axis as measured from the lateral x rays, and the angle at which the maximum target strength of the same fish was measured. The slope of the line was not significantly different from 1 (slope=1,  $p > 0.10$ , power=0.93).

standard length of the fish in cm ( $F_{SL}$ ) and its dorsal aspect target strength [Fig. 5(a)]. Some differences were evident between species. The pink snapper had the steepest slope in the relationship between log of standard length and dorsal target strength ( $TS = 20.6 * \log(F_{SL}) - 55.1$ ,  $r^2 = 0.85$ ). The red snapper ( $TS = 13.7 * \log(F_{SL}) - 46.6$ ,  $r^2 = 0.54$ ) and long-tailed red snapper ( $TS = 12.6 * \log(F_{SL}) - 42.9$ ,  $r^2 = 0.80$ ) had similar slopes but the long-tailed red snapper had target strengths that were about 2 dB higher for equivalently sized fish. The target strengths of the three individual snappers that were not target species fit the same general, length–target strength relationship.

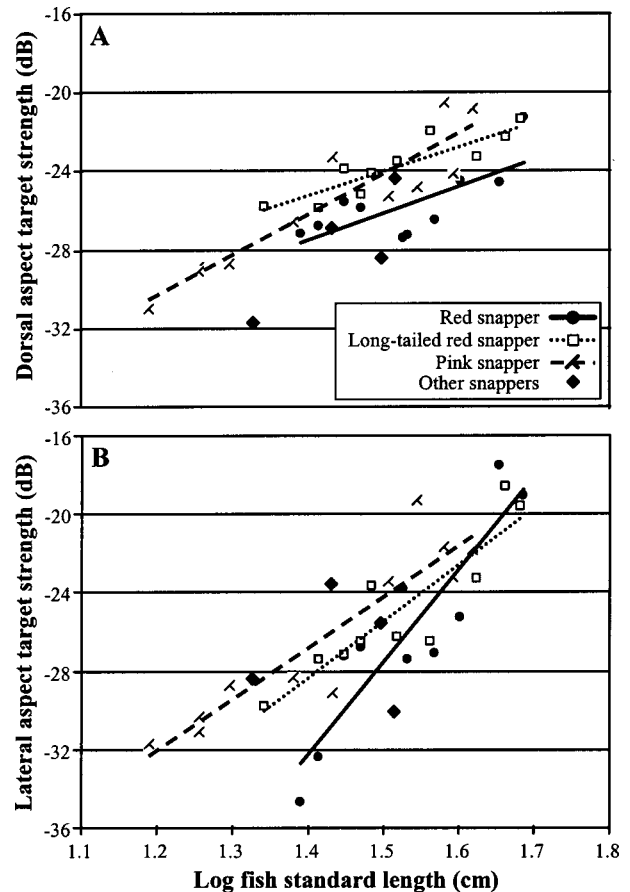


FIG. 5. Relationship between the standard length of each fish species and its dorsal-aspect (a) and lateral-aspect (b) target strength. *F*-tests reveal that the slopes of all lines are significant ( $p < 0.01$ ).

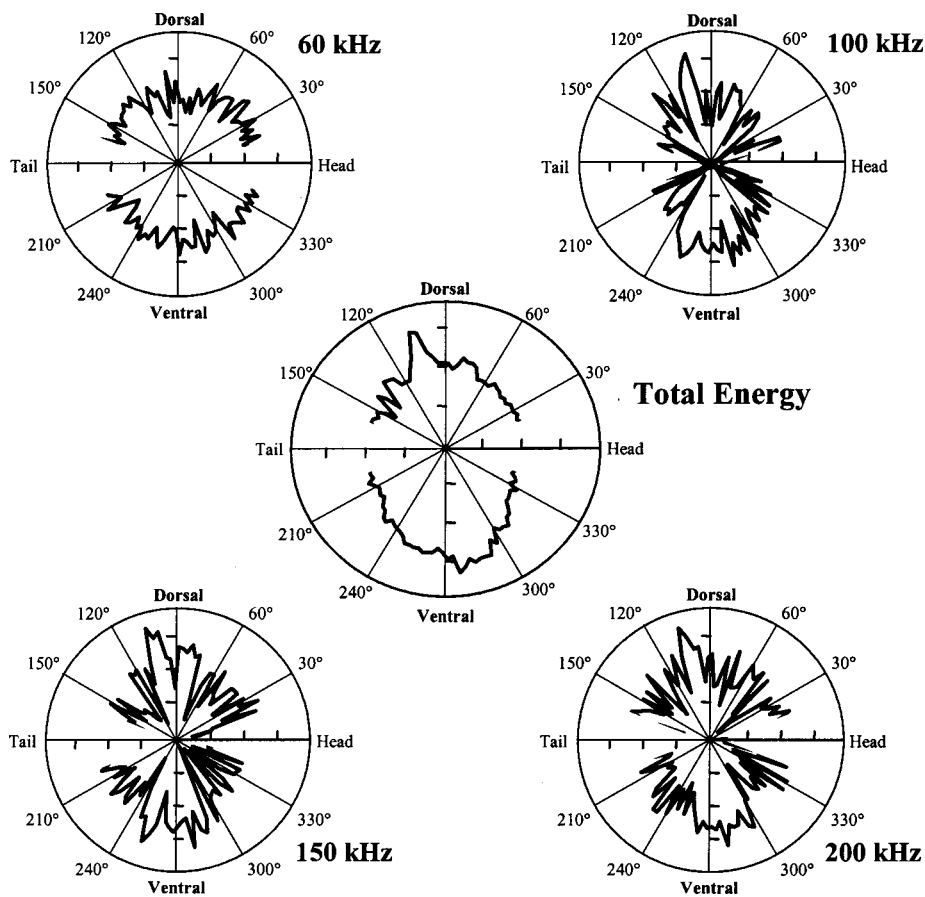


FIG. 6. Target strength as a function of dorsal tilt angle for a 41-cm-long pink snapper. The total energy target strength is shown in the center, surrounded by the target strength at discrete frequencies. The target strengths are scaled to the maximum observed for the fish. Each tick mark represents a loss of 10 dB from the maximum value, up to 35 dB below the maximum value. Echoes taken from within 15° of the head and tail of the fish were dominated by the mounting rig and are not shown.

For the three primary species, there was also a strong, linear relationship between the log of the fish's standard length and its lateral aspect target strength ( $p < 0.05$  for all comparisons) [Fig. 5(b)]. The relationship between the length and the pink snapper's lateral aspect target strength could be described by the equation  $TS = 26.2 * \log(F_{SL}) - 63.5$  ( $r^2 = 0.85$ ). The red snapper had the steepest slope in the relationship between log of standard length and target strength ( $TS = 47.2 * \log(F_{SL}) - 98.3$ ,  $r^2 = 0.81$ ). The long-tailed red snapper's lateral aspect target strength-length relationship can be described as  $TS = 28.9 * \log(F_{SL}) - 68.8$  ( $r^2 = 0.81$ ).

Consistent effects of frequency on the target strength of fish were not observed. Other studies have found that target strength decreases with increasing frequency, specifically by 0.9 log frequency (see Love, 1969, 1970; Urick, 1983). While the range of variation in target strength as a function of frequency was approximately the same as that predicted by this equation, no consistent change was observed as a function of frequency. Essentially, the log length-target strength regression lines for each frequency cross both in the dorsal and lateral aspect.

The variance in target strength as a function of the fish's orientation for the entire rotation in each plane increased with increasing frequency for all species (Fig. 6). Variance values increased from 13 to 49  $\text{dB}^2$  with increasing frequency. The total energy target strength variance, with values between 0.1 to 11  $\text{dB}^2$ , was lower than the variance of all discrete frequencies, in all three planes. Differences in the magnitude of target strength variance as a function of angle

were observed between species (Fig. 7). In the tilt plane, the red snapper had a larger variance than the other species. In the roll plane, the red snapper had a lower variance than the other species, although the overall variance for all three species in this plane was low. The variance in the lateral plane was much higher in the pink snapper than in the other species; both the red and long-tailed red snappers had very low variance in this plane.

The  $\pm 15^\circ$  about both the dorsal and lateral aspects of the fish are the most important for utilizing these measures in a field study. The variance over the  $\pm 15^\circ$  about each major axis was generally decreased compared with the variance over the entire fish. Species differences in the magnitude of variance in target strength about the tilt and lateral axes were evident. However, there were no differences in variance between species in the roll plane over this limited range of angles; the variance in target strength of all three species was extremely low. The target strength over this range of angles had a range of 8 to 12 dB in the tilt plane, 2.5 to 7 dB in the roll plane, and 4 to 6 dB in the lateral plane. Single factor analysis of variance revealed that there were significant differences in the range of target strengths observed in all three planes as a function of species ( $p < 0.05$ ). Long-tailed red snapper had the greatest range of target strength values in the tilt plane and the most limited range of target strength values in the roll and lateral planes. Red snapper and pink snapper had similar ranges in their target strengths over the  $\pm 15^\circ$  about each major axis.

Dorsal-aspect acoustic backscattering cross section was linearly related to wet weight in grams, a measure of bio-

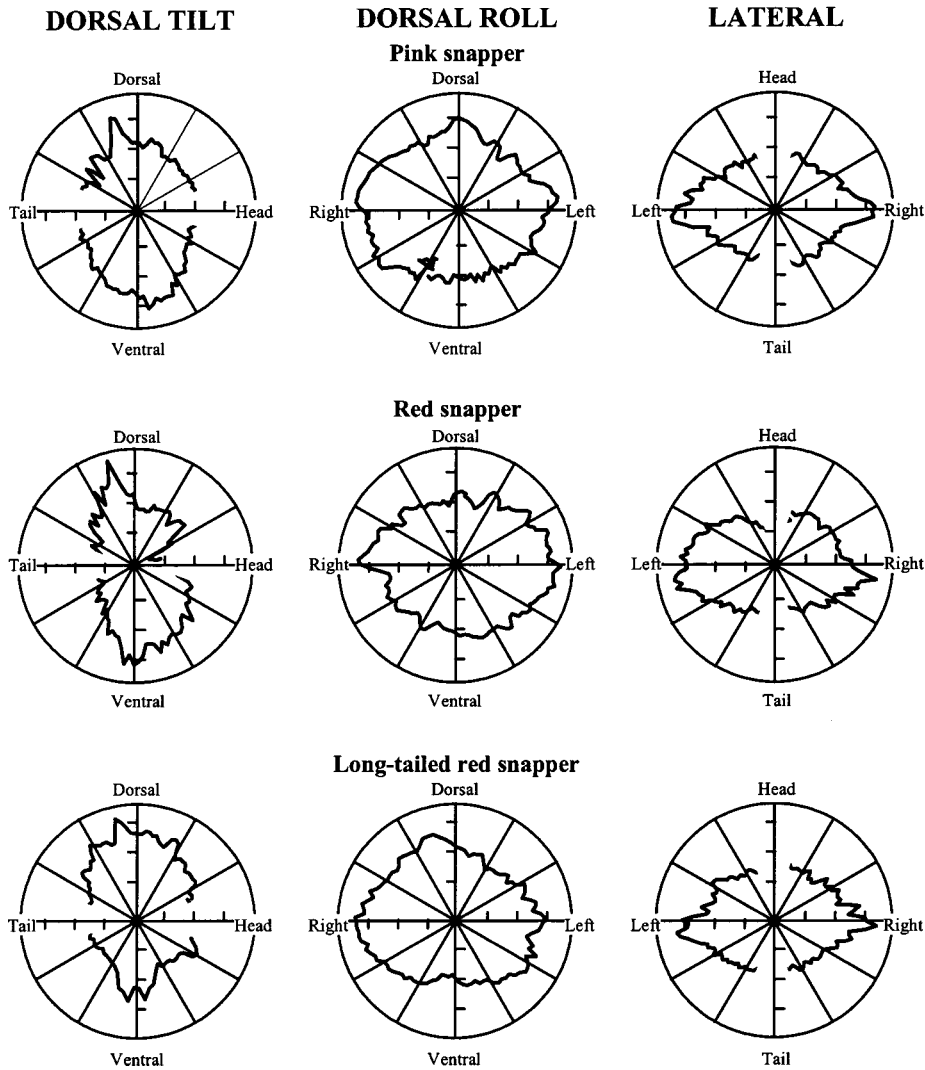


FIG. 7. Total energy target strength of a representative of each species of fish as a function of orientation. Dorsal tilt is shown on the left, dorsal roll in the center, and lateral aspect on the right. Each tick mark represents a loss of 10 dB from the maximum value, up to 35 dB below the maximum value. Echoes taken from within 15° of the head and tail of the fish were dominated by the mounting rig and are not shown.

mass, for each snapper species (Fig. 8) [red snapper wet weight ( $g$ ) =  $22983 \cdot \sigma(m^2) - 18.39$  ( $r^2 = 0.82$ ,  $p < 0.05$ ); long-tailed red snapper wet weight ( $g$ ) =  $24631 \cdot \sigma(m^2) - 527.55$  ( $r^2 = 0.71$ ,  $p < 0.05$ ); pink snapper wet weight ( $g$ ) =  $12665 \cdot \sigma(m^2) - 122.91$  ( $r^2 = 0.77$ ,  $p < 0.05$ )]. Similar relationships were observed between acoustic backscattering cross section and biovolume. Acoustic backscattering cross section did not predict biovolume and wet weight significantly differently than the cube of length, a standard predictor ( $p > 0.05$  for both comparisons). These relationships could be helpful in estimating fish biomass in future field studies of these species, without needing length-weight curves for each species (Benoit-Bird and Au, 2002).

### C. Models

Comparison between maximum measured target strength values and those predicted by various models for lateral and dorsal aspect target strength showed only the prolate spheroid model was accurate and precise (Fig. 9). The predictions from the sphere model, based on the volume of

the swimbladder, were significantly different from both the lateral aspect and dorsal aspect target strength ( $p < 0.005$ ). Both target strength models using fish length, based on the

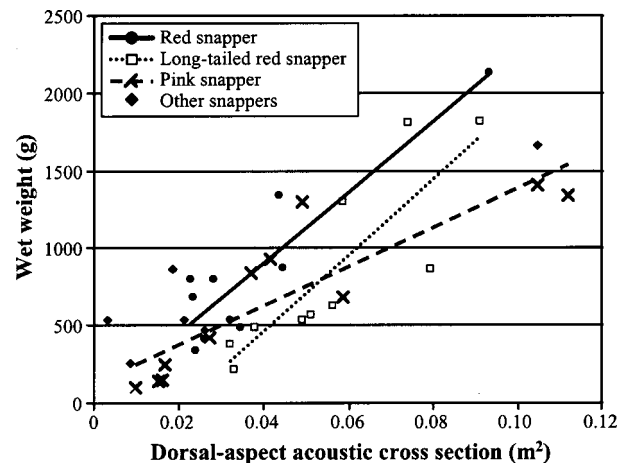


FIG. 8. The relationship between the dorsal-aspect acoustic cross-section and biomass, expressed as wet weight. There is a strong relationship and a significant slope ( $p < 0.05$ ).

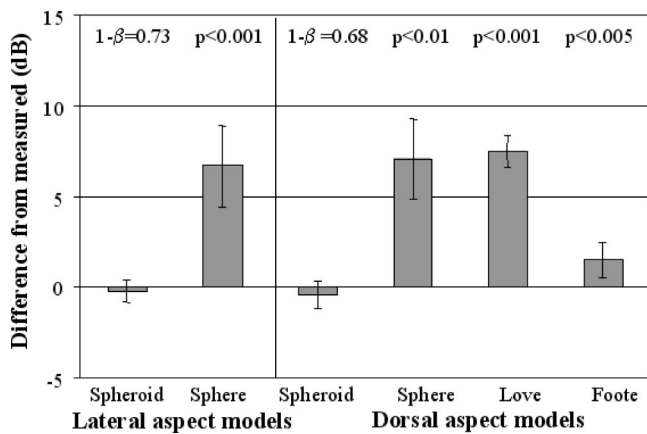


FIG. 9. Comparison between measured target strength values and those predicted by various models. Lateral aspect models, one modeling the swimbladder as a prolate spheroid based on the axes of the swimbladder measured from an x ray, and one modeling the swimbladder as a sphere with a volume equivalent to that measured of a plaster cast of the swimbladder. The dorsal aspect models are shown on the right; again the prolate spheroid and sphere models for target strength based on the swimbladders are included as are the models based on fish length for all types of fish (Love, 1970) and only on fish possessing a swimbladder (Foote, 1980). Positive values indicate that the model, on average, underestimated the fish's target strength and negative values indicate the model overestimated the fish's target strength. Error bars show 95% confidence intervals. The  $p$  values are indicated for models that differ significantly from the data, compared with paired  $t$ -tests corrected for multiple comparisons using the Bonferroni method. Power values are shown for the models that are not significantly different from the data.

equations of Love (1970) and Foote (1980), predicted values that were significantly different than the maximum dorsal aspect target strength ( $p < 0.005$ ). Foote's equation for fish with air-filled swimbladders predicted maximum target strength significantly better than the general fish equation of Love ( $p < 0.05$ ). The target strengths predicted by the prolate spheroid model of the swimbladder were not significantly different from the maximum measured target strengths from either the dorsal or lateral aspects (power=0.73). The measured target strengths were all within 3 dB of the predictions of the prolate spheroid model.

On average, the lateral aspect target strength was 0.8 dB higher than the dorsal aspect target strength of the same fish. The relationship is reversed in more than one-third of the individuals, with the dorsal aspect target strength being higher than the lateral, unlike the trend that is commonly observed (Love, 1969). In all fish, the prolate spheroid model correctly predicted which aspect should have the higher target strength, if not the difference between the two. However, it is important to note that the target strength values used here are based on energy over a 60-kHz band while values for the other models were at a specific frequency.

#### IV. DISCUSSION

X rays and swimbladder casts revealed that the swimbladder shapes among different snapper species varied significantly. This is evidenced in the percent of body length of the three swimbladder axes. The differences are visible in the swimbladder x rays where differences are particularly noticeable in the degree of curvature or linearity of the swimblad-

ders. Interestingly, the fish in the genus *Pristimopoides*, closely related fish, showed remarkable differences in their swimbladder shapes. Likewise, the swimbladder characteristics of two fish species in the genus *Etelis* were very different. The fish within each genus were more different from each other than some of the other, less related fish. This is obvious in the swimbladder volume, expressed as percent of body volume. The differences in volume between fish are greater within each genus than between them.

While swimbladder shape and volume varied between species, target strength values among the three target species did not greatly vary. Target strengths, both lateral and dorsal, of all three target species were correlated with standard length. The lateral aspect target strength was predicted about equally well by standard length in all three species. The dorsal aspect target strength was predicted equally in the long-tailed red snapper and the pink snapper. However, the relationship between length and lateral aspect target strength was weaker in the red snapper. The relationship between fish length and the axes of the fish swimbladders was strong in both the long-tailed red snapper and pink snappers, with  $r^2$  values greater than 0.75 for the major and minor axes of the swimbladders, and greater than 0.44 for the vertical axis. However, the red snapper had a strong correlation between length and only the major axis of the swimbladder ( $r^2 = 0.83$ ). There was no significant relationship between red snapper length and the length of the minor or vertical axes of its swimbladders ( $r^2 < 0.14$ , slope  $\neq 0$ ,  $p > 0.15$ , power=0.48). Because swimbladder size is a primary factor responsible for the strength of echoes, this lack of a correlation between two of the swimbladder size measures and length translates to a weaker relationship between red snapper length and target strength.

Swimbladder shape in all three target species varied most in the dorso-ventral plane. Changes in swimbladder shape were particularly noticeable in fish with full stomachs. Because the dorsal aspect cross-sections of the swimbladders varied less than the lateral-aspect cross sections, variance in the lateral-aspect target strength between individuals within a species was greater than target strength variance in the dorsal aspect. Variance in target strength within individuals about the lateral axis was also high. Consequently, attempts to estimate snapper size from target strength when fish cannot be directly observed would be more accurate from the dorsal than the lateral aspect, suggesting the most appropriate tool for field surveys would be a downward-looking sonar system or upward-looking, bottom-mounted devices.

The lack of a relationship between frequency and target strength is contrary to previous work. Other studies have found that target strength decreases with increasing frequency ( $f$ ), specifically by  $0.9 \log(f)$  (Love, 1969, 1970; Urick, 1983). This is caused by the complex relationship between target strength and frequency within each fish, discussed in Au and Benoit-Bird (2003).

As expected, the directivity of target strength values over each plane of the fish increased with increasing frequency (Urick, 1983) and contained many nulls and local peaks. However, the broadband, total energy target strength had the lowest directivity. The broadband pattern based on

total energy was considerably smoother than the patterns at the various frequencies. Local maxima and minima in the narrow-band pattern are the results of constructive and destructive interferences of the scattered signals. The interference effect is not as strong with broadband signals. Utilizing the broadband target strength of these fish could reduce the error associated with estimating their size when they have an unknown distribution of tilt and roll angles. Differences between species in the directivity of target strength, particularly within 15° of the dorsal axis, can introduce differences in this error, assuming an equivalent distribution of orientations. The use of broadband target strength estimates would reduce the differences.

A strong correlation between the dorsal aspect acoustic backscattering from each of the three target snapper species and their wet weight, a measure of biomass, was observed. This permits a direct conversion of acoustic backscattering to biomass without knowledge of the size distribution of the population (Benoit-Bird and Au, 2002). While some differences in the relationship were observed between species, the combined relationship for all three species was still strong ( $r^2=0.65$ ,  $p<0.05$ ). This could permit a conversion of acoustic scattering to snapper species biomass, even if specific species identification were not possible.

Modeling acoustic backscattering strength using measures of fish physical characteristics can elucidate the factors affecting sound scattering. The prolate spheroid model of Furusawa (1988) accurately predicted the maximum target strengths of all species of snappers, based only on simple size characterization of the swimbladder. The model also accurately predicted the direction of differences between dorsal and lateral-aspect target strength. None of the other models used, based on fish length or swimbladder volume, accurately predicted target strength. It is likely that the Clay and Horne model based on fish swimbladder shape would accurately predict target strength, however the complexities involved in calculating the model were beyond the scope of this work. Models based on fish length varied in their ability to predict target strength in different species because of small species-specific differences in length–target-strength relationship. Both the Love and Foote models use total fish length as the predictive variable. The relationships between fish total length and target strength were significantly weaker for all three species than the relationships between fish standard length, a measure of only the firm tissue of the fish ignoring the tail, and target strength ( $p<0.05$  for all comparisons). This indicates that variance in fish target-strength–length relationships could be reduced by utilizing standard length instead of total length. The prolate spheroid model showed no differences in its ability to predict target strength. Unlike the other models of target strength used, the prolate spheroid model overestimated the target strength of the fish. This is likely because of the simple swimbladder shape assumed by the model and the contribution of the rest of the fish’s body to the backscattering. The accuracy and generality of the predictions of target strength based on these simple measures of swimbladder size, however, indicate the importance of the swimbladder in the echo strength of these fish. This is confirmed by the correlation between swimbladder

tilt angle and the angle of maximum reflection.

Few detailed studies of acoustic backscattering strength by a group of closely related fish have been reported. The questions of frequency, orientation, biomass, and the relationship between swimbladder shape, orientation, and size were investigated utilizing a combination of techniques. Specific target-strength–length and backscattering–biomass relationships were determined for the three most abundant snapper species. The effect of frequency on scattering strength was unpredictable, unlike previous results. Orientation effects on backscattering strength show the potential of broadband target strength measures to reduce errors associated with an unknown distribution of fish orientation in the wild. The results of target strength models based on x ray measures of swimbladder characteristics indicate the importance of the shape of a snapper’s swimbladder size on its backscattering strength. These results also provide an important base for the utilization of sonar techniques for field studies of snappers in the Hawaiian Islands.

## ACKNOWLEDGMENTS

Aaron and Virginia Moriwake maintained the fish while in the hatchery, and assisted in the capture of the fish from the hatchery, design of the fish mounting setup, and data collection. Bo Alexander caught the fish from the wild, assisted in their maintenance, and captured fish from the hatchery for study. More than this, however, they shared their knowledge of the fish, anesthesia techniques, and their enthusiasm for the Bottomfish Project as a whole. Romeo Estabilio and the Queen’s Hospital Imaging Department generously donated their time, expertise, and materials to provide all of the fish x rays. Kristine Hiltunen, a student in the National Science Foundation’s Research Experience for Undergraduates Program, assisted in data collection and processing. Kimberly Andrews and Caroline DeLong assisted in data collection. Jeff Pawloski provided valuable information regarding x-ray facilities. This work was supported by the Hawaii State Department of Land and Natural Resources. This is HIMB contribution 1166.

- Au, W. W. L., and Benoit-Bird, K. J. (2003). “Acoustic backscattering by Hawaiian lutjanid snappers. II. Broadband temporal and spectral structure,” *J. Acoust. Soc. Am.* **114**, 2767–2774.
- Benoit-Bird, K. J., and Au, W. W. L. (2002). “Energy: Converting from acoustic to biological resource units,” *J. Acoust. Soc. Am.* **111**, 2070–2075.
- Benoit-Bird, K. J., Au, W. W. L., Kelley, C. D., and Taylor, C. (2003). “Acoustic backscattering from deepwater measured in situ from a manned submersible,” *Deep-Sea Res., Part I* **50**, 221–229.
- Clay, C. S., and Horne, J. K. (1994). “Acoustic models of fish: The Atlantic cod (*Gadus morhua*),” *J. Acoust. Soc. Am.* **96**, 1661–1668.
- Do, M. A., and Surti, A. M. (1990). “Estimation of dorsal aspect target strength of deep-water fish using a simple model of swimbladder backscattering,” *J. Acoust. Soc. Am.* **87**, 1588–1596.
- Foote, K. G. (1980). “Importance of the swimbladder in acoustic scattering by fish: A comparison of gadoid and mackerel target strengths,” *J. Acoust. Soc. Am.* **67**, 2084–2089.
- Foote, K. G., and Ona, E. (1985). “Swimbladder cross sections and acoustic target strengths of 13 pollack and 2 saithe,” *Fiskeridirektoratets* **18**, 1–57.
- Furusawa, M. (1988). “Prolate spheroidal models for predicting general trends of fish target strength,” *J. Acoust. Soc. U. K.* **9**, 13–24.

- Love, R. H. (1969). "Maximum side-aspect target strength of an individual fish," *J. Acoust. Soc. Am.* **3**, 746–752.
- Love, R. H. (1970). "Dorsal-aspect target strength of an individual fish," *J. Acoust. Soc. Am.* **49**, 816–823.
- MacLennan, D. N. (1990). "Acoustical measurement of fish abundance," *J. Acoust. Soc. Am.* **87**, 1–15.
- McClatchie, S., Alsop, J., and Coombs, R. F. (1996). "A re-evaluation of relationships between fish size, acoustic frequency, and target strength," *ICES J. Mar. Sci.* **53**, 780–791.
- Ona, E. (1990). "Physiological factors causing natural variations in acoustic target strength of fish," *J. Mar. Biol. Assoc. U.K.* **70**, 107–127.
- Stanton, T. K. (1989). "Simple approximate formulas for backscattering of sound by spherical and elongated objects," *J. Acoust. Soc. Am.* **86**, 1499–1510.
- Thiebaux, M. L., Boudreau, P. R., and Dickie, L. M. (1991). "An analytical model of acoustic fish reflection for estimation of maximum dorsal aspect target strength," *Can. J. Fish. Aquat. Sci.* **48**, 1772–1782.
- Urick, R. J. (1983). *Principles of Underwater Sound* (McGraw–Hill, New York).
- Western Pacific Regional Fisheries Management Council (1999). "Bottom-fish and Seamount Ground fish of the Western Pacific Region, 1998," Annual Report.